Available online at www.sciencedirect.com
SCIENCE DIRECT
Earth and Planetary Science Letters 242 (2006) 143–154
EPSL
www.elsevier.com/locate/epsl

Oscillations in land surface hydrological cycle

D. Labat *

Laboratoire de Mécanisme de Transfert en Géologie, UMR 5563 CNRS/IRD/UPS, 14 Avenue Edouard Belin, 31400 Toulouse, France

Received 18 March 2005; received in revised form 15 November 2005; accepted 28 November 2005
Available online 9 January 2006
Editor: V. Courtillot

Abstract

Hydrological cycle is the perpetual movement of water throughout the various component of the global Earth's system. Focusing on the land surface component of this cycle, the determination of the succession of dry and humid periods is of high importance with respect to water resources management but also with respect to global geochemical cycles.

This knowledge requires a specified estimation of recent fluctuations of the land surface cycle at continental and global scales. Our approach leans towards a new estimation of freshwater discharge to oceans from 1875 to 1994 as recently proposed by Labat et al. [Labat, D., Goddéris, Y., Probst, JL, Guyot, JL, 2004. Evidence for global runoff increase related to climate warming. Advances in Water Resources, 631–642]. Wavelet analyses of the annual freshwater discharge time series reveal an intermittent multiannual variability (4- to 8-y, 14- to 16-y and 20- to 25-y fluctuations) and a persistent multidecadal 30- to 40-y variability.

Continent by continent, reasonable relationships between land–water cycle oscillations and climate forcing (such as ENSO, NAO or sea surface temperature) are proposed even though if such relationships or correlations remain very complex.

The high intermittency of interannual oscillations and the existence of persistent multidecadal fluctuations make prediction difficult for medium-term variability of droughts and high-flows, but lead to a more optimistic diagnostic for long-term fluctuations prediction.

Keywords: global hydrologic cycle; wavelet analysis; climate variability; multidecadal oscillation

Oscillations in the global climate system are usually tracked by an extensive analysis of the fluctuations of parameters such as pressure or temperature (continental and sea surface temperature). Above others, two main signals are well known from the scientific community and have major impacts on global climate:

- ENSO: a sea surface temperature fluctuation observed over the Tropical Pacific that impacts precipitation in many locations around the globe from South America to Africa, Australia and North America [2].
- NAO (North Atlantic Oscillation): this North Atlantic sea-level pressure Oscillation exerts a considerable influence on the hydroclimatology of Europe, Northern America and Canada [3–5].

Indeed, only a few signals are directly related to the continental water cycle. What kind of signal can be considered as a valuable record of the continental water cycle? Two signals may be of interest: precipitation and discharge records.

Precipitation time series are intermittent signals that can not be easily analyzed and are only representative of a very restricted area.

Indeed, river draining areas larger than 10^5 km^2 integrate rainfall, evaporation, topography, lithology

* Tel.: +33 5 61 33 26 12; fax: +33 5 61 33 25 60.
E-mail address: labat@lmtg.obs-mip.fr.

0012-821X/$ - see front matter © 2005 Elsevier B.V. All rights reserved.
doi:10.1016/j.epsl.2005.11.057

and vegetation heterogeneities thus integrating regional climatic fluctuations [6]. Hence, it seems reasonable to consider stream flows of large rivers as consistent proxies to perform global and long-term (from 10 to 100 y) analyses.

Several previous studies already show interannual or multidecadal variability in large river runoffs all over the world ([7–13] among others). However, these oscillations and trends are only representative of regional climate and an integrated signal representative of land surface water cycle is still lacking.

1. Continental freshwater discharge to oceans

This issue has been recently overcome by Labat et al. [1]. Using a wavelet-based estimation method applied to the annual discharges of 221 worldwide large rivers, the temporal variations of annual continental and global freshwater discharge have been recently estimated over the 1875–1994 interval.

The database includes 221 rivers: 66 in North America including the St Lawrence, Colorado, Columbia, Ohio, Nelson and Mac Kenzie; 51 in Asia including the Mekong, Amur, Ob, Yenisey, Lena, Chang Jiang and Volga; 40 in Europe including the Danube, Northern Dvina and Elbe; 33 in South America including the Amazone, Parana, Orinoco and Tocantins and 31 in Africa including the Nile, Congo, Niger and Zambezi. The surface area of the gauging reference stations ranges from 10^4 km^2 to $4.5*10^6$ km^2.

The reader is highly incited to refer to Labat et al. [1] (Tables 1, 2 and 3) for a complete description including the length of the discharge records and the geographical localization of the gauge stations. Gauge stations where streamflow is measured are located in Fig. 1.

Leading to the same results as Peterson et al. [20] Artic river discharges analysis, land surface runoff fluctuations reveal a rate of increase of 8% per year over the last 75 y. However, this increasing rate must be qualified at continental scale with a 14.3% increase over North America contrasting with a mean 2% decrease over Africa and Europe. Therefore, the regression analysis of global land surface runoff against global temperature from 1925 to 1994 exhibits a positive 4% increase and then correlates for the first time the intensification of the water cycle to global warming at continental and global scale [15].

In this paper, we focus on the oscillations that may be detected in these global hydrological signals and relate periodicities to already mentioned ones in the

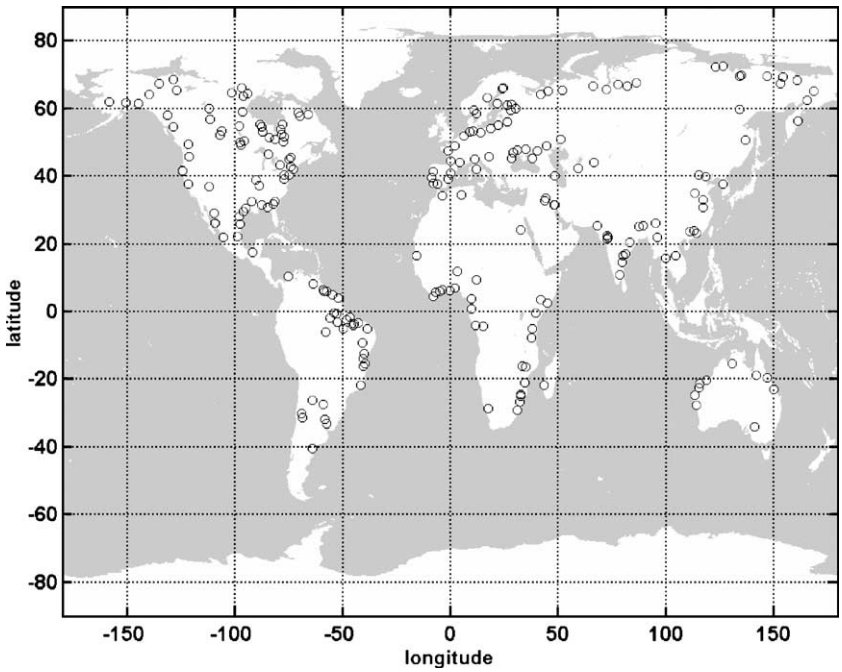

Fig. 1. Geographical location of the 231 stations considered in the continental and global runoff reconstruction process. Spatial repartition of the gauging stations appears homogeneous and globally follows the latitudinal distribution of continents, given that 46 rivers are located in the southern hemisphere and 185 rivers in the northern hemisphere. Surface area of the gauging reference stations ranges from 10^4 km^2 to $4.5*10^6$ km^2, latitude and longitude position range respectively from 40.3 S to 72.37 N and −158.1 W to 184 E.

literature (especially in sea surface temperature time series since sea surface temperature fluctuations control the amount of water available over continental area).

2. Spectral analysis

In a first time, the classical spectral analysis is applied to these global hydrological signals. The power spectrum density of the global discharge signals corresponds to the Fourier transform of the correlation function (Wiener Kinchine theorem). It allows to determine the characteristic periods and oscillations in global discharge signals (Fig. 2).

- Africa continental runoff displays interannual 7- to 8-y, 16-y and 40- to 50-y oscillation.
- Asia continental runoff displays interannual 5- to 6-y and multidecadal 30-y oscillations,
- Europe continental runoff displays interannual 4- to 5-y, 14-y and multidecadal 25- and 50-y oscillations,

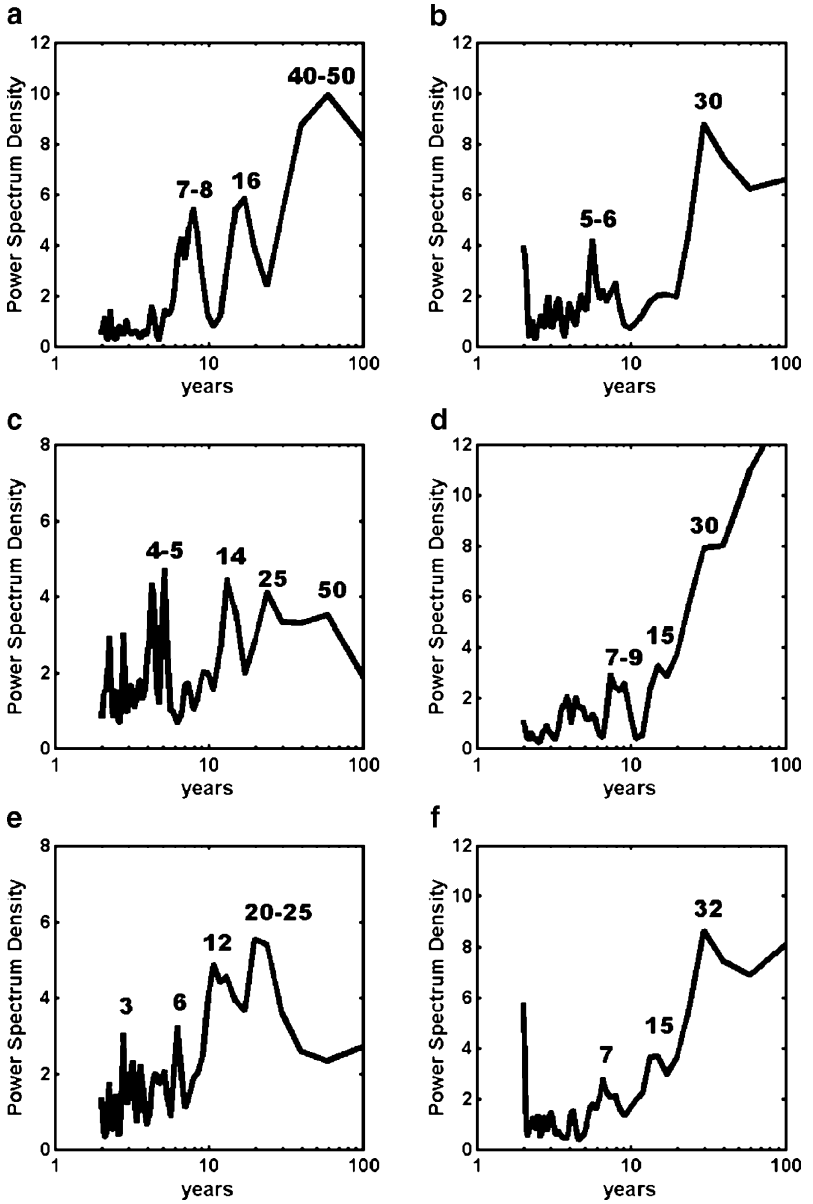

Fig. 2. Spectral analysis of the global and continental discharge signals obtained by Labat et al. [1]. It allows a first identification of the characteristic oscillations in land surface runoff over the last century (a—Africa runoff, b—Asia runoff, c—Europe runoff, d—North America runoff, e—South America runoff and f—Global continental runoff).

- North America continental runoff displays 7- to 9-y, 15-y and 30-y oscillation,
- South American continental runoff displays interannual 3- and 6-y oscillations and 12-y and 20- to 25-y processes.

Finally, global continental discharge displays 7-y, 15-y and a dominant multidecadal 32-y process. Then, Fourier analysis allows a preliminary determination of the characteristic periods in land surface runoff and already identify interannual, decadal and multidecadal oscillations. These results are now corroborated introducing wavelet analysis that constitutes a most robust method when dealing with non-stationary signals.

3. Morlet continuous wavelet transform

Because of their non-stationarity, Benner et al. [14] has already emphasized the wavelet analysis ability to show that "most of the climatic oscillations are non-stationary and do not persist for the entire span of the time series". From the large number of techniques currently available [16], the powerful wavelet analysis is much preferred to the classical Fourier analysis, because of the natural non-stationarity of hydrological series [17]. In hydrology, several applications of wavelet to stream flow time series have already been presented for North America [21,22], for South America [14,18,23], for Africa [11] and for Europe [19].

The basic objective of the continuous wavelet transform is to achieve a complete time-scale representation of localized and transient phenomena's occurring at different time scales. The coefficients of the wavelet transform of a continuous-time signal $x(t)$ are defined by the linear integral operator:

$$C_x(a,\tau) = \int_{-\infty}^{+\infty} x(t)\psi_{*a,\tau}(t)dt \quad \text{with}$$
$$\psi_{a,\tau}(t) = \frac{1}{\sqrt{a}}\psi\left(\frac{t-\tau}{a}\right) \tag{1}$$

where * corresponds to the complex conjugate. The function $\psi(t)$, which can be either real or complex, acts as a convolution-kernel and is called a wavelet. The parameter "a" can be interpreted as a dilation ($a>1$) or contraction ($a<1$) factor of the wavelet function $\psi(t)$, corresponding to different scales of observation. The parameter "τ" can be interpreted as a temporal translation or shift of the function $\psi(t)$, which allows the study of the signal $x(t)$ locally around the time τ. Wavelet analysis then allows to distinguish intermittent oscillations (located over a restricted time interval) from persistent oscillations (corresponding to a horizontal line in the wavelet spectrum).

The wavelet spectrum $W_x(a,\tau)$ of a continuous-time signal $x(t)$ is defined, by analogy with the Fourier analysis, by

$$W_x(a,\tau) = C_x(a,\tau)C_x^*(a,\tau) = |C_x(a,\tau)|^2 \tag{2}$$

This wavelet spectrum can also be averaged in time, referred to as the global averaged wavelet power spectrum, but at the cost of an information loss [24].

The determination of the characteristic periods of oscillation is achieved using the global wavelet spectrum. Two statistical limits are considered in order to restrict our analysis to statistically significant-only fluctuations:

- Only periodicity different from red noise is taken into consideration and 95% and 90% confidence intervals are depicted in the figures following Torrence and Campo [24] calculations.
- Due to the edge effects leading to the presence of a cone of influence, if T is the total length of the series, only periods smaller than $T/(2\sqrt{2})$ are considered as significant.

4. Pulses and oscillations in the land surface hydrological cycle

The aim of this study remains to identify the most energetic periods that affect continental freshwater to oceans. Of course, continental discharge integrates a large number of rivers with different regimes.

For example, South American river basins such as Amazon are controlled by ENSO whereas Arctic and European rivers are mainly under Artic Oscillation or NAO influence. The hydrological regimes of Siberian rivers such as the Ob, Lena or Yenisey also strongly differ from the Mekong tropical basin.

Indeed, since climate forcing generally operates at different scales, if a climatic forcing strongly impacts a large region but not all a continent, the wavelet analysis of the continental freshwater time series identifies such periodicity. Hence, only the most remarkable periodicities remain identified.

Hence, the question remains: what are the major and most influent climate periodicities of the global land surface water cycle?

4.1. Africa freshwater discharge wavelet analysis

African continental runoff wavelet spectrum (Fig. 3) displays intermittent 7.5-y ENSO-related interannual processes around 1915 and from 1960 to 1980. This

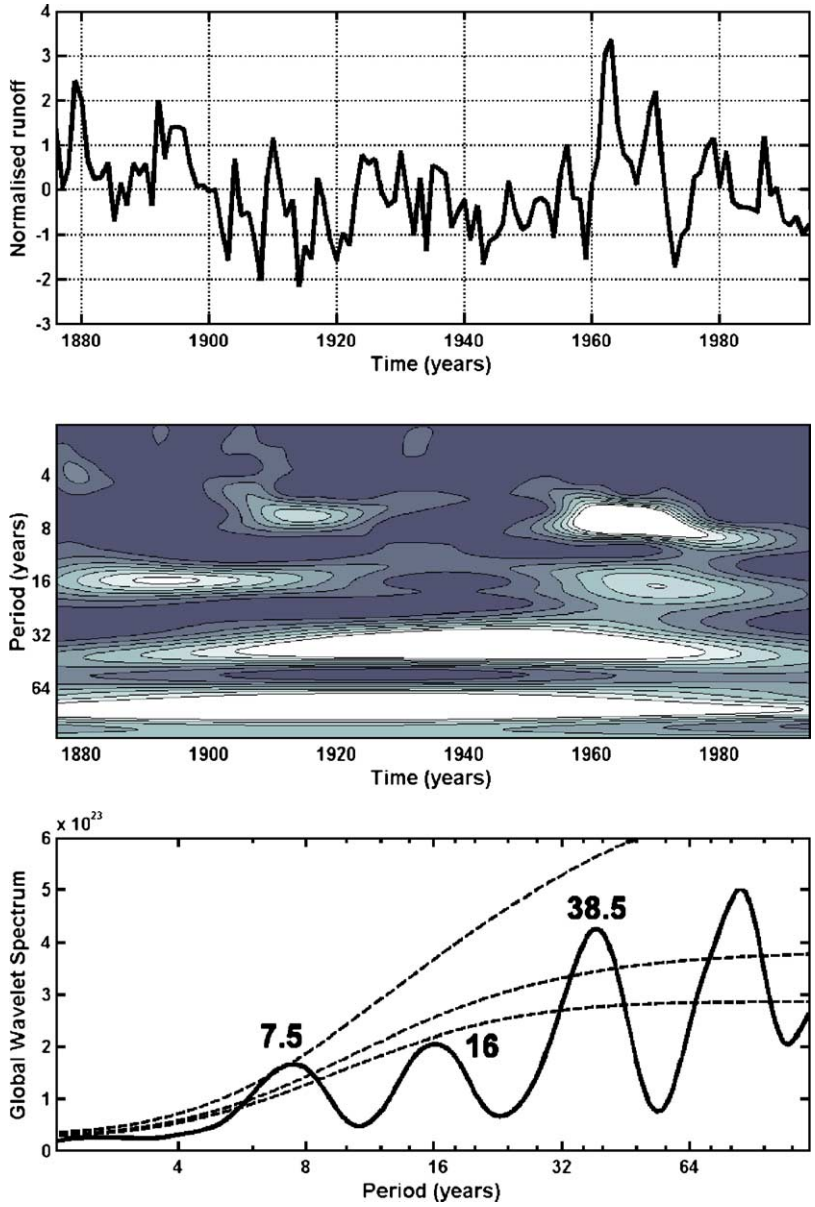

Fig. 3. Morlet wavelet analysis of Africa annual freshwater discharge to ocean fluctuations from 1875 to 1994. From top to bottom: temporal fluctuations of continental discharge, two-dimensional Morlet wavelet spectrum and global wavelet spectrum and global Morlet wavelet spectrum. The dashed line corresponds to the 95%, 90% and 80% statistical confidence interval from red noise [note that estimation of annual continental discharge is based on 31 African rivers including the Nile, Congo, Niger and Zambezi].

interannual oscillation is generally associated to ENSO fluctuations or tropical Atlantic sea surface temperature fluctuations [25,26]. It may also be related to South Atlantic sea surface temperature fluctuations [27].

Then, the wavelet analysis also shows intermittent 16-y fluctuations from 1875 to 1920 and from 1958 to 1982. A similar 13- to 15-y oscillation has already been mentioned by Venegas et al. [27] and Wainer and Venegas [28] in singular value decomposition of South Atlantic sea surface temperature time series.

Finally, considering multidecadal scales, African continental discharge exhibits persistent 38.5 y as highlighted in South Atlantic sea surface temperature time series [28].

4.2. Asia freshwater discharge wavelet analysis

Asia annual runoff wavelet spectrum (Fig. 4) shows low-intensity but statistically significant 6-y ENSO-related interannual variability from 1935 to 1950 corresponding to the Pacific coast rivers. Persistent

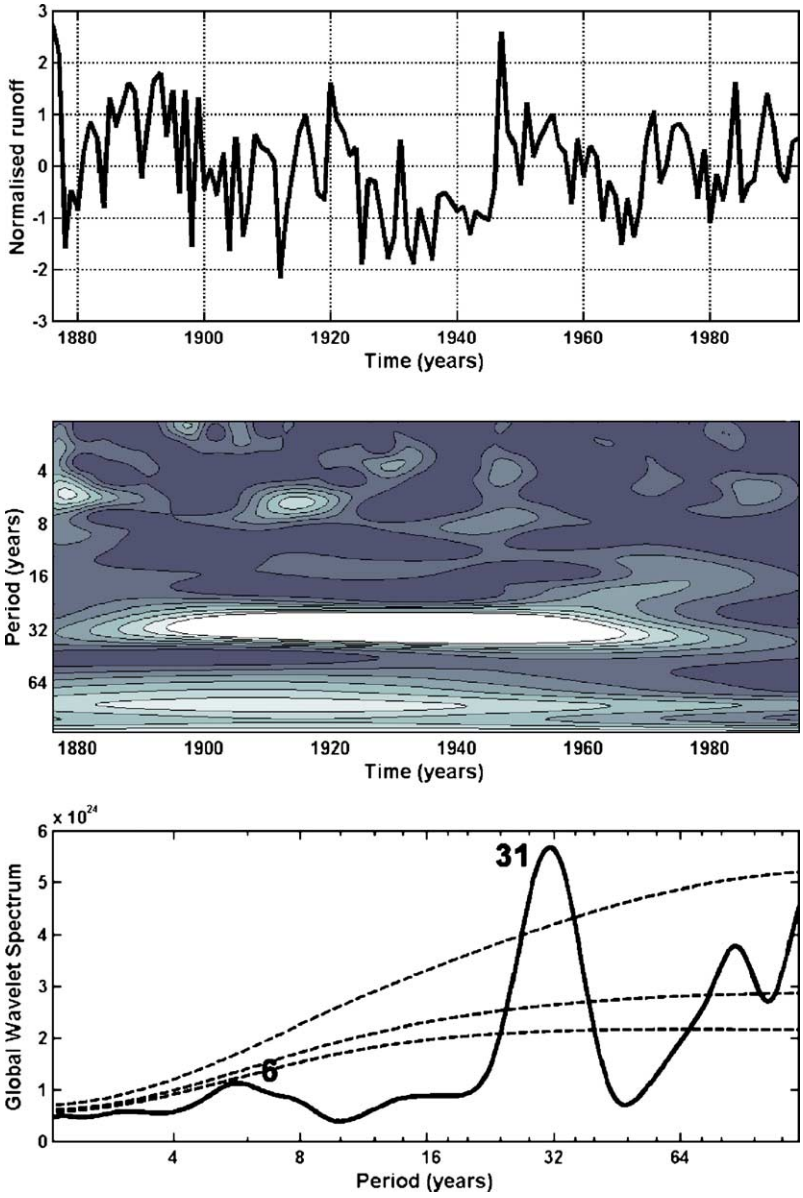

Fig. 4. Morlet wavelet analysis of Asia annual freshwater discharge to ocean fluctuations from 1875 to 1994. From top to bottom: temporal fluctuations of continental discharge, two-dimensional Morlet wavelet spectrum and global wavelet spectrum and global Morlet wavelet spectrum. The dashed line corresponds to the 95%, 90% and 80% statistical confidence interval from red noise [note that estimation of annual continental discharge is based on 51 Asian rivers including the Mekong, Amur, Ob, Yenisey, Lena, Chang Jiang and Volga].

31-y oscillation appears as restricted from 1875 to 1960. The most energetic oscillation remains the 31-y oscillation. Such oscillation may be related to the already documented 30- to 50-y Artic Oscillation variability [29] that impacts over the Artic rivers.

4.3. Europe freshwater discharge wavelet analysis

At interannual scales, Europe runoff wavelet spectrum (Fig. 5) highlights intermittent 4- to 5-y interannual processes and 13-y oscillation from 1920 to 1970. Multidecadal fluctuation is identified after 1935 with a decreasing period varying from 28 to 23 y. It must be noted that it is consistent with Lucero and Rodriguez [30] Morlet wavelet analysis of European rainfall variability exhibiting a 20- to 22-y NAO-related bidecadal component. Finally, a pentadecadal oscillation is highlighted from 1900 to 1980.

Oscillations appear as closely related to the two major climate fluctuations that impacts Europe: the

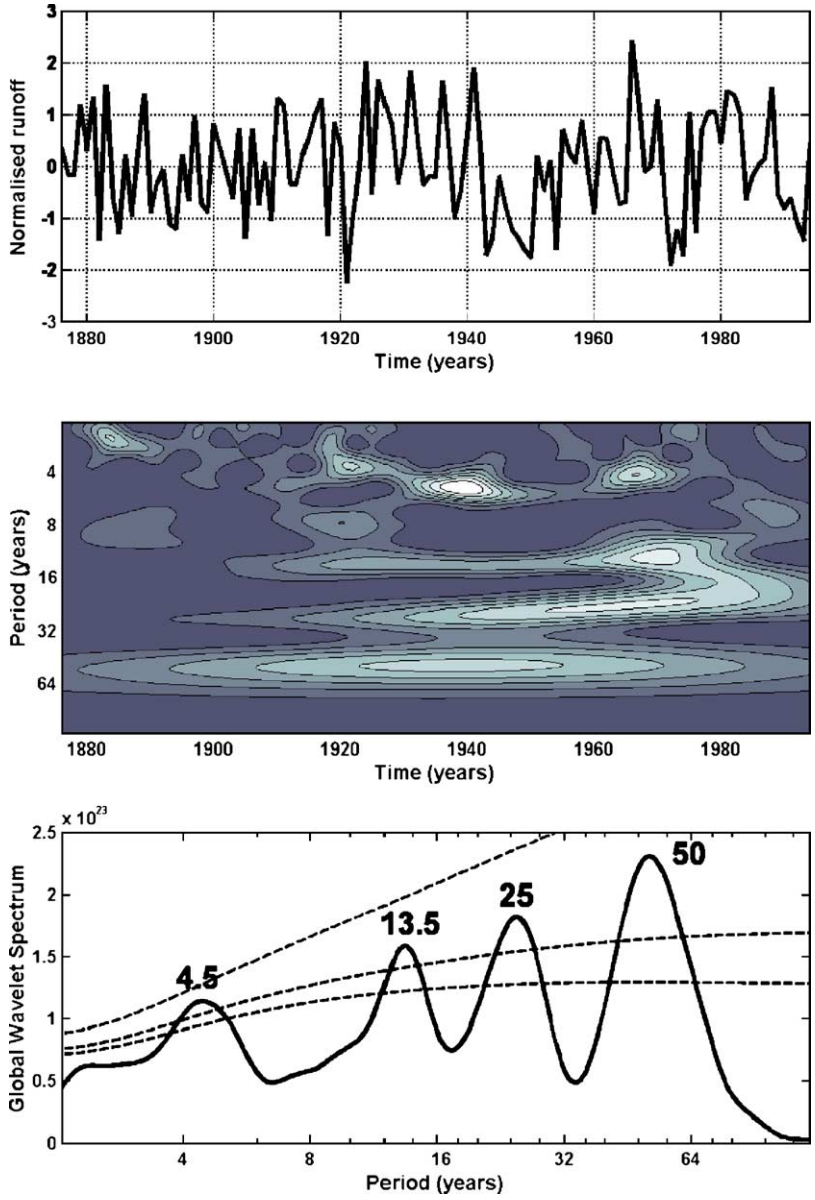

Fig. 5. Morlet wavelet analysis of Europe annual freshwater discharge to ocean fluctuations from 1875 to 1994. From top to bottom: temporal fluctuations of continental discharge, two-dimensional Morlet wavelet spectrum and global wavelet spectrum and global Morlet wavelet spectrum. The dashed line corresponds to the 95%, 90% and 80% statistical confidence interval from red noise [note that estimation of annual continental discharge is based on 40 European rivers including the Danube, Northern Dvina and Elbe].

North Atlantic Oscillation [31] and the Artic Oscillation that exhibit multidecadal variability and impact principally western Europe [29].

4.4. North America freshwater discharge wavelet analysis

North America annual discharge wavelet spectrum (Fig. 6) displays a 4- to 8-y intermittent low-intensity processes. Sun and Furbish [32] already reported a correlation between river discharges of Florida and ENSO at interannual scale in accordance with the 4–8-y oscillation. Over the central part of the continent, Lucero and Rodriguez [33] also find in precipitation fields an interannual mode related to ENSO phenomenon.

At longer time scales, several components are highlighted: a 24-y oscillations observed after 1930 and a persistent 34-y fluctuations. This is also in accordance

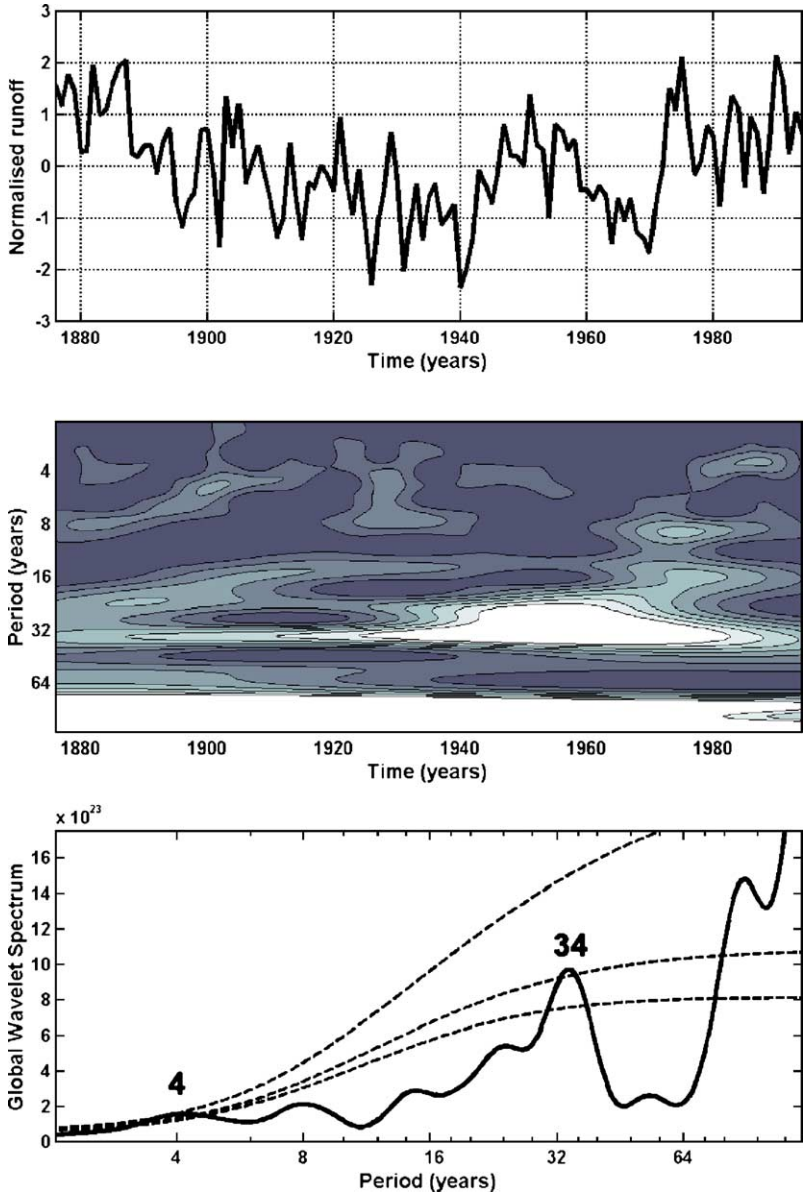

Fig. 6. Morlet wavelet analysis of North America annual freshwater discharge to ocean fluctuations from 1875 to 1994. From top to bottom: temporal fluctuations of continental discharge, two-dimensional Morlet wavelet spectrum and global wavelet spectrum and global Morlet wavelet spectrum. The dashed line corresponds to the 95%, 90% and 80% statistical confidence interval from red noise [note that estimation of annual continental discharge is based on 66 North American rivers including the St Lawrence, Colorado, Columbia, Ohio, Nelson and Mac Kenzie].

with Lucero and Rodriguez [33] and Currie and Fairbridge [34] reports of a bidecadal 21- to 22-y oscillation in precipitation fields. At multidecadal scales, Gray et al. [35] also highlight 20-y and 30- to 70-y variability in drought fluctuations extrapolated from tree-ring records.

The 25- to 30-y and the 50-y oscillation emphasized over North America may be related to the North Atlantic Oscillation since reconstructions based on tree-ring studies exhibit 24-, and 50- to 70-y long-term variability [36–38]. These oscillations may also be related to the Pacific Decadal Oscillation (PDO), since wavelet analyses show two major spectral bands: 15- to 25-y and 50- to 70-y [39–41].

4.5. South America freshwater discharge wavelet analysis

South America runoff wavelet spectrum (Fig. 7) is mainly characterized by intermittent interannual pro-

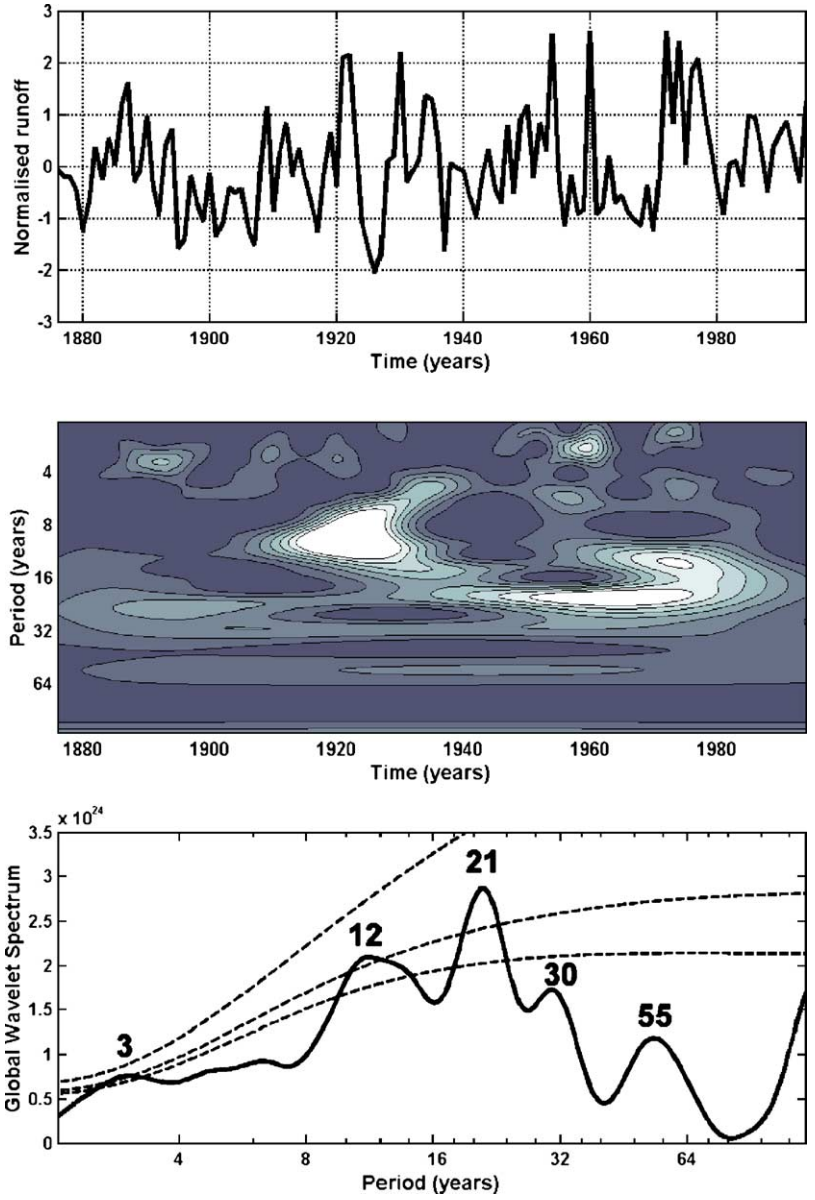

Fig. 7. Morlet wavelet analysis of South America annual freshwater discharge to ocean fluctuations from 1875 to 1994. From top to bottom: temporal fluctuations of continental discharge, two-dimensional Morlet wavelet spectrum and global wavelet spectrum and global Morlet wavelet spectrum. The dashed line corresponds to the 95%, 90% and 80% statistical confidence interval from red noise [note that estimation of annual continental discharge is based on 33 South American rivers including the Amazon, Parana, Orinoco and Tocantins].

cesses with periods ranging from 3- to 7-y. Then, wavelet spectrum identifies a 12-y variability already observed in rainfall fields [33].

The 21-y bidecadal fluctuation detected in South America annual runoff has also already been shown in precipitation fields [23,33].

At multidecadal scales, the persistent 30-y oscillations has been previously described by Krepper and Sequeira [42] and Lucero and Rodriquez [33] rainfall analysis. Moreover, a similar 30-y multidecadal variability is shown over the Amazon basin [12,13].

The interannual variability may be directly related to ENSO mode but should also be related to both Pacific and Atlantic teleconnections [7,23,43,44]. The bidecadal oscillation [39,45,46] constitutes the major fluctuation over South America land surface

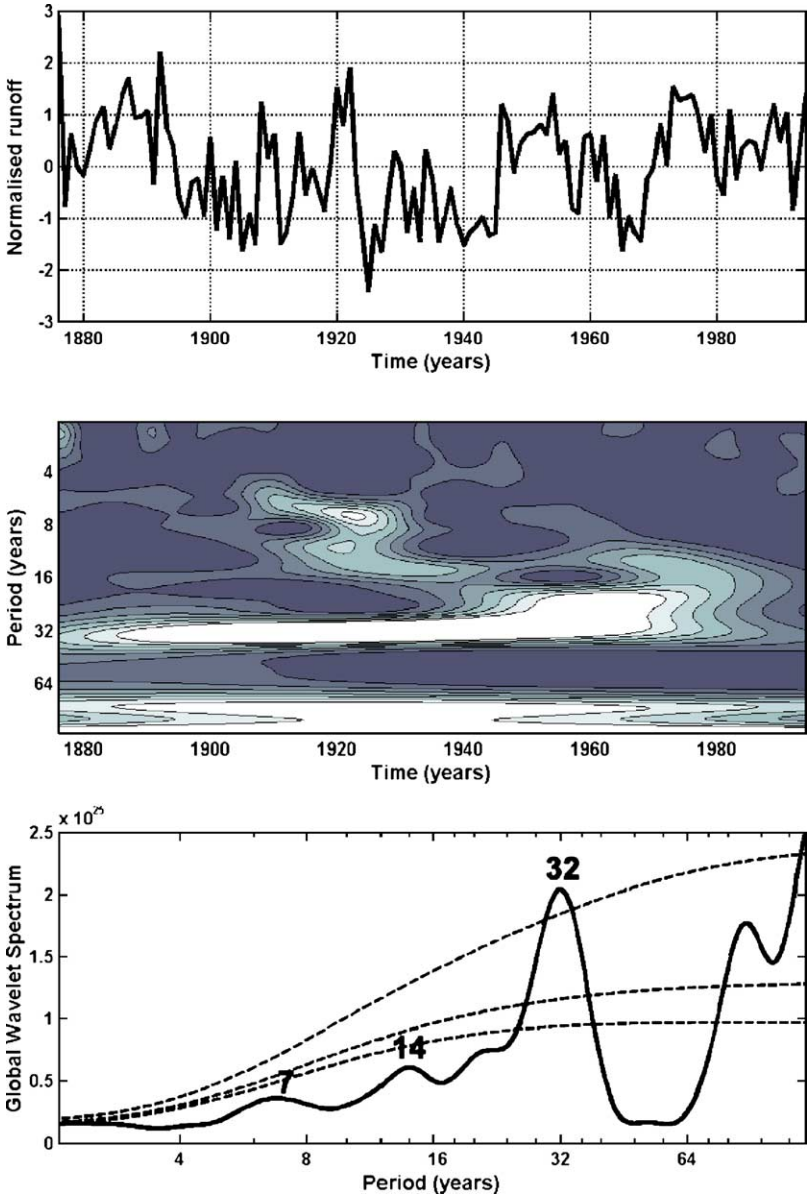

Fig. 8. Morlet wavelet analysis of the Global annual freshwater discharge to ocean fluctuations from 1875 to 1994. From top to bottom: temporal fluctuations of continental discharge, two-dimensional Morlet wavelet spectrum and global wavelet spectrum and global Morlet wavelet spectrum. The dashed line corresponds to the 95%, 90% and 80% statistical confidence interval from red noise.

runoff. This runoff oscillation may be related to South Atlantic sea surface temperature and sea level pressure fluctuations [27].

4.6. Global water discharge to the oceans

At global scale (Fig. 8), the wavelet spectrum of annual freshwater discharge to oceans displays 7-y interannual fluctuations combined with 14-y variability. As mentioned for Asia, North America and South America, the 32-y persistent variability remains the major fluctuation.

5. Discussion

At interannual scale, 4- to 8-y ENSO-related and 6- to 8-y NAO-related variability are highlighted in continental land surface hydrological cycles.

At interdecadal scale, a global 14- to 16-y oscillation is identified but should be qualified at continental scale

Table 1
Summary of the characteristic periods shown by spectral and wavelet analyses in continental and global freshwater discharge to oceans based on Labat et al. [1] data

Continent	Characteristic periods	
	Spectral analysis	Wavelet analysis
	y	y
Africa	7–8, 16, 40–50	7, 16, 38
Asia	5–6, 30	6, 31
Europe	4–5, 14, 25, 50	4–5, 13, 25, 50
North America	7–9, 45, 30	4, 34
South America	3, 6, 12, 20–25	3, 15, 21
GLOBAL	7, 15, 32	7, 14, 32

as a 13.5-y NAO- or AO-related oscillation over Europe, a 14-y NAO-related variability over North America and a 11.3-y ENSO-related variability over South America. The decadal variability already mentioned in North and Tropical Atlantic sea surface temperature series [47–49] is not clearly highlighted.

Europe and North America land surface runoffs highlight a 25- to 35-y variability probably associated to global oceanic thermohaline circulation [50,51] or to the Pacific Decadal Variability which exhibits 15- to 25-y fluctuations [52].

At multidecadal scale, wavelet analyses show a large range of variability from 30- to 40-y oscillations in Asia, Africa and South America annual land surface hydrological cycle and a 50-y oscillation in Europe and South America annual land surface hydrological cycle. Such pentadecal oscillation has already been observed by Minobe [40,41] in global sea level pressure and air temperature, whereas multidecadal oscillation in South America and Asia land surface hydrological cycle may be respected related to ENSO long-term variability and to PDO variability which exhibit 50 to 70 y.

6. Conclusions

In this paper, an insightful analysis of the fluctuations of the continental freshwater discharge to oceans over the last century is exposed. Based on spectral and wavelet analysis, this analysis highlights multi-scale oscillations and exhibits significant differences both in terms of spatial organization and temporal persistence (Table 1).

Land surface hydrological cycle over the last century strengthens the evidence for intermittent multiannual oscillations that can not be considered as persistent processes but should be rather considered as spatially and temporally localized pulses. Land surface hydrological cycle reveals an intermittent multiannual variability (4- to 8-y, 14- to 16-y and 20- to 25-y fluctuations) and a persistent multidecadal 30- to 40-y variability. These oscillations have been correlated to already known climate forcings and are consistent with already known sea surface temperature or pressure fluctuations (ENSO, NAO, PDO or AO among others). Hence, the global hydrological signals exposed in Labat et al. [1] are both in accordance in term of trends [16] but also integrate all the major climate disturbances.

The high intermittency of interannual oscillations and the existence of persistent multidecadal fluctuations make prediction difficult for medium-term variability of droughts and high-flows, but lead to a more optimistic diagnostic for long-term fluctuations prediction.

References

[1] D. Labat, Y. Goddéris, J.L. Probst, J.L. Guyot, Evidence for global runoff increase related to climate warming, Adv. Water Resour. (2004) 631–642.
[2] C.F. Ropelewski, M.S. Halpert, Global and regional scale precipitation patterns associated with the El Niño/Southern Oscillation, Mon. Weather Rev. (1987) 1606–1626.
[3] J.C. Rogers, The association between the North Atlantic Oscillation and the Southern Oscillation in the Northern Hemisphere, Mon. Weather Rev. 112 (1984) 1999–2015.
[4] J. Hurell, W. van Loon, Decadal variations in climate associated with the North Atlantic Oscillation, Clim. Change 36 (1996) 301–326.
[5] J. Marshall, Y. Kushnir, D. Battisti, P. Chang, A. Czaja, R. Dickson, J. Hurell, M. McCartney, R. Saranavan, M. Visbeck, North Atlantic climate variability: phenomena, impacts and mechanisms, Int. J. Climatol. 21 (2001) 1863–1898.
[6] J.L. Probst, Y. Tardy, Long range streamflow and world continental runoff fluctuations since the beginning of this century, J. Hydrol. 94 (1987) 289–311.
[7] G. Berri, M.A. Ghietto, N.O. Garcia, The influence of ENSO in the flows of the upper Parana river of South America over the past 100 years, J. Hydrol. 3 (2002) 57–65.
[8] H. Bjornsson, L.A. Mysak, R.D. Brown, On the interannual variability of precipitation and runoff in the MacKenzie drainage basin, Clim. Dyn. 12 (1) (1995) 67–76.
[9] P.J. Depetris, S. Kempe, M. Latif, W.G. Mook, ENSO controlled flooding in the Parana's river 1904–1991, Nature 83 (1996) 127–129.
[10] E.A.B. Eltahir, El Niño and the natural variability in the flow of the Nile River, Water Resour. Res. 32 (1) (1996) 131–137.
[11] M.R. Jury, J-L. Melice, Analysis of Durban rainfall and Nile river flow 1871–1999, Theor. Appl. Climatol. 67 (2000) 161–169.
[12] D. Labat, J. Ronchail, J. Callède, J.L. Guyot, E. De Oliveira, W. Guimarães, Wavelet analysis of Amazon hydrological regime variability, Geophys. Res. Lett. 31 (2004) L02501.
[13] L.C. Smith, D.L. Turcotte, B.L. Isacks, Stream flow characterization and feature detection using a discrete wavelet transform, Hydrol. Process. 12 (1998) 233–249.
[14] T.C. Benner, Central England temperatures: long term variability and teleconnections, Int. J. Climatol. 19 (1999) 391–403.
[15] T.G. Huntington. Evidence for intensification of the global water cycle: review and synthesis. Journal of Hydrology (in press).

[16] M. Ghil, M.R. Allen, M.D. Dettinger, K. Ide, D. Kondrashov, M.E. Mann, A.W. Robertson, A. Saunders, Y. Tian, F. Varadi, P. Yiou, Advanced spectral methods for climatic time series, Rev. Geophys. 40 (1) (2000) 1–41.
[17] D. Labat, R. Ababou, A. Mangin, Rainfall–runoff relations for karstic springs: Part II. Continuous wavelet and discrete orthogonal multiresolution analyses, J. Hydrol. 238 (2000) 149–178.
[18] J. Marengo, Variations and change in South American streamflow, Clim. Change 31 (1995) 99–117.
[19] P. Pekarova, P. Miklanek, J. Pekar, Spatial and temporal runoff oscillation analysis of the main rivers of the world during the 19th–20th centuries, J. Hydrol. 274 (2003) 62–79.
[20] B.J. Peterson, R.M. Holmes, J.W. McClelland, C.J. Vörösmarty, R.B. Lammers, A.I. Shiklomanov, I.A. Shiklomanov, S. Rahmstorf, Increasing river discharge to the Artic Ocean, Science 298 (2002) 2171–2173.
[21] M. Lafrenieres, M. Sharp, Wavelet analysis of inter-annual variability in the runoff regimes of glacial and nival stream catchments, Bow Lake, Alberta, Hydrol. Process. 17 (6) (2003) 1093–1118.
[22] P. Coulibaly, D.H. Burn, Wavelet analysis of variability in annual Canadian streamflows, Water Resour. Res. 40 (3) (2004) W03105, doi:10.1029/2003WR002667.
[23] R.H. Compagnucci, S.A. Blanco, M.A. Figliola, P.M. Jacovkis, Variability in subtropical Andean Argentinean Atuel river: a wavelet approach, Environmetrics 11 (2000) 251–269.
[24] C. Torrence, G.P. Compo, A practical guide to wavelet analysis, Bull. Am. Meteorol. Soc. 79 (1998) 61–78.
[25] S.E. Nicholson, D. Entekhabi, The quasi-periodic behaviour of rainfall variability in Africa and its relationship to the Southern Oscillation, J. Clim. Appl. Meteorol. 34 (1986) 311–348.
[26] S.E. Nicholson, The nature of rainfall variability over Africa on time scales of decades to millenia, Glob. Planet. Change 26 (2000) 137–158.
[27] S.A. Venegas, L.A. Mysack, D.N. Straub, Evidence for interannual and interdecadal climate variability in the South Atlantic, Geophys. Res. Lett. 23 (1996) 2673–2676.
[28] I. Wainer, S.A. Venegas, South Atlantic multidecadal variability in the Climate System Model, J. Climate 12 (2002) 1408–1420.
[29] D.W.J. Thompson, J.M. Wallace, The Arctic Oscillation signature in the wintertime geopotential height and temperature fields, Geophys. Res. Lett. 25 (1998) 1297–1300.
[30] O.A. Lucero, N.C. Rodriguez, Spatial organisation in Europe of decadal and interdecadal fluctuations in annual rainfall, Int. J. Climatol. 22 (2002) 805–820.
[31] C. Shorthouse, N.W. Arnell, Spatial and temporal variability in European river flows and the North Atlantic Oscillation. FRIEND'97, Int. Assoc. Hydrol. Sci. Pub. 246 (1997) 77–85.
[32] H. Sun, D.J. Furbish, Annual precipitation and river discharges in Florida in response to El Nino- and La Nina-sea surface temperature anomalies, J. Hydrol. 199 (1997) 74–87.
[33] O.A. Lucero, N.C. Rodriguez, Spatial organization of decadal and bidecadal rainfall fluctuations in southern North America and Southern South America, Atmos. Res. 57 (2001) 219–246.
[34] R.G. Currie, R.W. Fairbridge, Periodic 18.6-year and cyclic 11-year signals in northeastern United States precipitation data, J. Climate 8 (1986) 228–255.
[35] S.T. Gray, J.L. Betancourt, C.L. Fastie, S.T. Jackson, Patterns and sources of multidecadal oscillations in drought sensitive tree-ring records from the central and southern Rocky Mountains, Geophys. Res. Lett. 30 (6) (2003) 1316, doi:10.1029/2002GL016154.
[36] J.W. Hurrell, Decadal trends in the North Atlantic Oscillation and relationships to regional temperature and precipitation, Science 269 (1995) 676–679.
[37] E.R. Cook, R.D. D'Arrigo, K.R. Briffa, A reconstruction of the North Atlantic Oscillation using tree-ring chronologies from North America and Europe, Holocene 8 (1998) 9–17.
[38] J. Luterbacher, C. Schmutz, D. Gyalistras, E. Xoplaki, H. Wanner, Reconstruction of monthly NAO and EU indices back to AD 1675, Geophys. Res. Lett. 26 (1999) 2745–2748.
[39] S. Minobe, N. Mantua, Interdecadal modulation of interannual atmospheric and oceanic variability over the North Pacific, Prog. Oceanogr. 43 (1999) 163–192.
[40] S. Minobe, A 50–70 years climatic oscillation over the North Pacific and North America, Geophys. Res. Lett. 24 (1997) 683–686.
[41] S. Minobe, Spatio-temporal structure of the pentadecadal variability over the North Pacific, Prog. Oceanogr. 47 (2000) 381–408.
[42] C.M. Krepper, M.E. Sequeira, Low frequency variability of rainfall in southeastern South America, Theor. Appl. Climatol. 61 (1998) 19–28.
[43] A.W. Robertson, C. Mechoso, Interannual and decadal cycles in river flows of southeastern South America, J. Climate 11 (1998) 2570–2581.
[44] I.A. Camilloni, V.R. Barros, The Parana river response to El Nino 1982–83 and 1997–98 events, J. Hydrometeorol. 1 (2000) 412–430.
[45] T.C. Royer, High latitude oceanic variability associated with the 18.6 year nodal tide, J. Geophys. Res. 98 (4) (1993) 639–644.
[46] M.E Mann, J. Park, R.S. Bradley, Global interdecadal and century-scale climate oscillations during the past five centuries, Nature 378 (1995) 266–270.
[47] V.M. Mehta, T. Delworth, Decadal variability of the tropical Atlantic Ocean surface temperature in shipboard measurements and in a global ocean-atmosphere model, J. Climate 8 (1995) 172–190.
[48] J.A. Carton, X. Cao, B.S. Giese, A.M. da Silva, Decadal and interannual SST variability in the tropical Atlantic, J. Phys. Oceanogr. 26 (1996) 1165–1175.
[49] P. Chang, L. Ji, H. Li, A decadal climate variation in the tropical Atlantic Ocean from thermodynamic air–sea interaction, Nature 385 (1997) 516–518.
[50] T.L. Delworth, S. Manabe, R. Stouffer, Interdecadal variability of the thermohaline circulation in a coupled ocean-atmosphere model, J. Climate 6 (1993) 1993–2011.
[51] T.L. Delworth, R.J. Greatbatch, Multidecadal thermohaline circulation variability driven by atmospheric surface flux forcing, J. Climate 13 (2000) 1481–1495.
[52] J.E. Overland, S. Salo, J.M. Adams, Salinity signature of the Pacific Decadal Oscillation, Geophys. Res. Lett. 26 (1999) 1337–1340.